

Chemosensory Performance of Molecularly Imprinted Fluorescent Conjugated Polymer Materials

Jiahui Li, Claire E. Kendig, and Evgueni E. Nesterov*

Department of Chemistry, Louisiana State University, Baton Rouge, Louisiana 70803

Received June 29, 2007; E-mail: een@lsu.edu

Abstract: Fluorescent conjugated polymers are an attractive basis for the design of low detection limit sensing devices owing to their intrinsic signal amplification capability. A simple and universal method to rationally control or fine-tune the chemodetection selectivity of conjugated polymer materials toward a desired analytical target would further benefit their applications. In a quest of such a method we investigated a general approach to cross-linked molecularly imprinted fluorescent conjugated polymer (MICP) materials that possess an intrinsic capability for signal transduction and have potential to enhance selectivity and sensitivity of sensor devices based on conjugated polymers. To study these capabilities, we prepared an MICP material for the detection of 2,4,6-trinitrotoluene and related nitroaromatic compounds. We found the imprinting effect in this material to be based on analyte shape/size recognition being substantial and generally overcoming other competing thermodynamically determined trends. The described molecularly imprinted fluorescent conjugated polymers show remarkable air stability and photostability, high fluorescence quantum yield, and reversible analyte binding and therefore are advantageous for sensing applications due to the ability to "preprogram" their detection selectivity through a choice of an imprinted template.

Introduction

The development of robust and sensitive platforms for real-time analytical detection is important in a broad range of practical areas. Fluorescence-based chemosensing, when analyte binding produces an attenuation in the light emission, has a remarkable advantage over other detection schemes due to its high sensitivity and detection simplicity.¹ Conjugated polymers (CPs) have found wide applications as a foundation for building fluorescent sensors.² The remarkable sensitivity of CP based sensor devices as compared to small molecule sensors is attributed to CPs' intrinsic ability to provide an amplified response to an analyte binding event.³ This amplification, first demonstrated by Swager in 1995,⁴ stems from the efficient energy transfer in CPs that allows excitation energy from large areas to be effectively funneled into the sites where analyte binding occurred. This effect is the most remarkable in aggregated systems and solid films, where it is greatly enhanced by intermolecular three-dimensional exciton migration via a Förster-type mechanism. It was previously demonstrated that the number of steps required for a randomly walking exciton to find a randomly distributed trap (analyte-bound site) with concentration c reduces from $1/c^2$ for a one-dimensional array

to $1/c$ for a three-dimensional network.⁵ This simple statistical reasoning alone can explain the greatly improved amplifying ability of CPs in the aggregated or solid state. The highest chemosensory efficiency of the CP based materials was found for the detection of electron-deficient analytes such as nitroaromatic compounds, which cause fluorescence quenching via the electron-transfer mechanism.⁶ Despite dramatic improvements in sensitivity, it still remains a challenging task to obtain a selective response toward a particular analyte, a condition that is required in order to reduce the false alarm rates of the detecting devices. It would be also conceivable to develop a simple and general way to change or fine-tune the chemodetection selectivity. The molecular shape of a target analyte is a natural feature that can be employed to achieve this goal through enhanced molecular recognition. This approach has been long and successfully used in molecular imprinting (MI), a versatile technique to create affinity in solid matrices through controlled selection of functional groups location and shape recognition.⁷ The idea of MI, as first put forward by Wulff⁸ and Mosbach,⁹

- (1) (a) Callan, J. F.; de Silva, A. P.; Magri, D. C. *Tetrahedron* **2005**, *61*, 8551–8588 and references therein. (b) Special issue on "Luminescent Sensors" *Coord. Chem. Rev.* **2000**, *205*, 1–232.
- (2) (a) McQuade, D. T.; Pullen, A. E.; Swager, T. M. *Chem. Rev.* **2000**, *100*, 2537–2574. (b) Thomas, S. W., III; Joly, G. D.; Swager, T. M. *Chem. Rev.* **2007**, *107*, 1339–1386. (c) Yang, C. J.; Pinto, M.; Schanze, K.; Tan, W. *Angew. Chem., Int. Ed.* **2005**, *44*, 2572–2576. (d) Liu, B.; Bazan, G. C. *J. Am. Chem. Soc.* **2006**, *128*, 1188–1196.
- (3) (a) Swager, T. M. *Acc. Chem. Res.* **1998**, *31*, 201–207. (b) Chen, L.; McBranch, D. W.; Wang, H.-L.; Helgeson, R.; Wudl, F.; Whitten, D. G. *Proc. Natl. Acad. Sci. U.S.A.* **1999**, *96*, 12287–12292.
- (4) Zhou, Q.; Swager, T. M. *J. Am. Chem. Soc.* **1995**, *117*, 12593–12602.

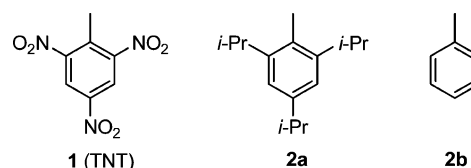
- (5) Montroll, E. W. *J. Phys. Soc. Jpn.* **1969**, *26* Suppl., 6–10.
- (6) (a) Yang, J.-S.; Swager, T. M. *J. Am. Chem. Soc.* **1998**, *120*, 11864–11873. (b) Yang, J.-S.; Swager, T. M. *J. Am. Chem. Soc.* **1998**, *120*, 5321–5322. (c) Sohn, H.; Sailor, M. J.; Magde, D.; Trogler, W. C. *J. Am. Chem. Soc.* **2003**, *125*, 3821–3830. (d) Liu, Y.; Mills, R. C.; Boncella, J. M.; Schanze, K. S. *Langmuir* **2001**, *17*, 7452–7455.
- (7) *Molecularly Imprinted Polymers: Man-Made Mimics of Antibodies and Their Applications in Analytical Chemistry*; Sellegren, B., Ed.; Elsevier: Amsterdam, 2001; (b) *Molecular and Ionic Recognition with Imprinted Polymers*; Bartsch, R. A.; Maeda, M., Eds.; ACS Symposium Series 703; American Chemical Society: Washington, DC, 1998. (c) Zimmerman, S. C.; Lemcoff, N. G. *Chem. Commun.* **2004**, 5–14. (d) Wei, S.; Jakusch, M.; Mizaikoff, B. *Anal. Chim. Acta* **2006**, *578*, 50–58.
- (8) Wulff, G.; Sarhan, A. *Angew. Chem., Int. Ed. Engl.* **1972**, *11*, 341.
- (9) Andersson, L.; Sellergren, B.; Mosbach, K. *Tetrahedron Lett.* **1984**, *25*, 5211–5214.

is very simple. A template with attached (covalently or noncovalently) functional monomers is copolymerized in the presence of cross-linking agents that results in formation of a polymer network around the template. Subsequent removal of the template leaves binding cavities that are complementary in shape and functionality to the template molecule. Although it has been long postulated that binding to the correctly preorganized functionalities inside the imprinted cavity plays a decisive role in selectivity of molecular imprinting, it has been recently demonstrated that it is the molecular shape which is crucially important in analyte recognition.¹⁰ This understanding opens up the prospect for obtaining high selectivity based on the shape recognition alone, therefore bringing about the possibility of preparing high recognition sites even for the analytes that lack specific binding groups.¹¹

The vast majority of MI methods uses “conventional” aliphatic, such as vinyl and acrylic, polymers. These traditional materials for MI generally show good selectivity but do not possess the ability for intrinsic signal transduction required for sensing applications.¹² To solve this dilemma, incorporating fluorescent dye reporters within the imprinted cavity of traditional molecularly imprinted polymers has been proposed.¹³ Still such materials suffer from low sensitivity. In contrast, the concept of **molecularly imprinted CPs (MICPs)** described herein utilizes CPs as **both** imprinting materials **and** analytical signal transducers. We presumed that, like typical fluorescent CPs, the MICP materials would possess high chemodetection sensitivity, coupled with the possibility of adjusting the detection selectivity by simply changing or modifying the template. Therefore, they could be considered as an interesting and general way to improve the selective response of CP based chemosensor materials.

At the time we initiated this research, there were only a few previous reports concerning studies on molecularly imprinted CPs. Cross-linked polypyrroles obtained by electropolymerization were most often used due to the convenience of this polymerization technique. In 1992, Sauvage et al. prepared a cross-linked polypyrrole matrix imprinted with metal cations.¹⁴ They demonstrated that removal of the cationic template resulted in a stable three-dimensional porous structure, which kept the “memory” of the template and could be recomplexed again. Since that milestone paper, there was some further development toward building sensors based on molecularly imprinted electropolymerized polypyrrole, polyphenol, poly(phenylenediamines), etc.¹⁵ In all the reports, electrochemical detection of analyte binding was used. To the best of our knowledge, there

were no systematic studies on using chemically synthesized fluorescent molecularly imprinted conjugated polymers, where more sensitive optical detection of analyte binding could be readily employed. We were naturally interested in filling this gap and studying the possibility of preparing fluorescent MICPs with the enhanced selectivity toward a particular analyte of choice. Since a common land-mine explosive 2,4,6-trinitrotoluene (TNT) **1** is a practical and desirable target for sensor design, we investigated the possibility of preparing “TNT-imprinted” fluorescent CPs and studied the properties of the resulting materials.¹⁶



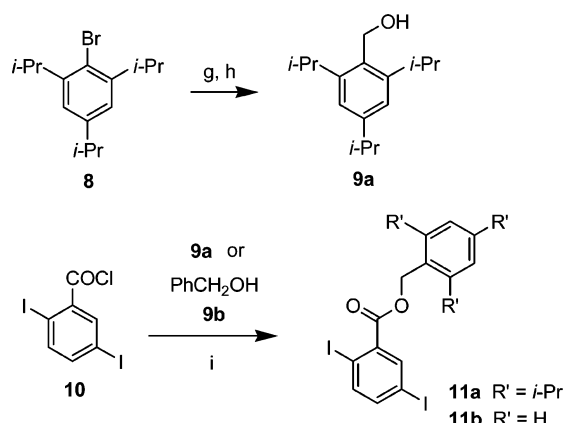
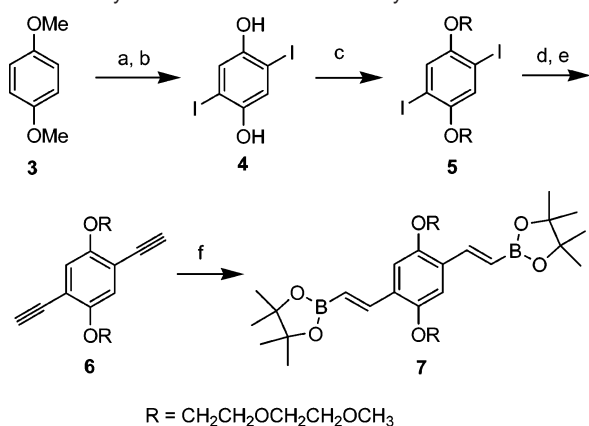
Results and Discussion

Preparation of MICP Materials. Three-dimensionally cross-linked poly(*p*-phenylene vinylene)s (PPVs) were a natural choice for the current study as they show some degree of conformational flexibility around the conjugated backbone that is required for shaping the imprinted cavity. In addition, PPVs are highly emissive in the solid state,¹⁷ and their fluorescent properties are strongly affected by the environment and the presence of quenchers.¹⁸ Three major components are necessary for preparing a molecularly imprinted material: a monomer, a cross-linker, and a template. As cross-linked polymers are not soluble, we paid special attention to the design of the synthetic strategy which would allow synthesis of these materials in a form suitable for further studies and applications.

Emulsion polymerization at a water–organic interface is a robust approach to prepare cross-linked micro- and nanoparticles of conjugated polymers.¹⁹ Suzuki coupling, although not widely used for PPV synthesis,²⁰ was preferred as it requires mild conditions. The synthesis of the monomers for polymerization, diiodide **5** and bis-vinylboronate **7**, is shown in Scheme 1. The *trans* bis-vinylboronate monomer **7** was prepared in good yield by using hydroboration of the precursor bis-acetylene **6**. We found that this reaction barely proceeds in the absence of catalyst

- (10) (a) Sibrían-Vázquez, M.; Spivak, D. A. *J. Am. Chem. Soc.* **2004**, *126*, 7827–7833. (b) Spivak, D. A.; Campbell, J. *Analyst* **2001**, *126*, 793–797.
- (11) As an example of highly selective molecular imprinting of a nonfunctionalized template, imprinting of hexachlorobenzene was recently reported: Das, K.; Penelle, J.; Rotello, V. M. *Langmuir* **2003**, *19*, 3921–3925.
- (12) (a) Dickert, F. L.; Forth, P.; Lieberzeit, P.; Tortschanoff, M. *Fresenius' J. Anal. Chem.* **1998**, *360*, 759–762. (b) Hillberg, A. L.; Brain, K. R.; Allender, C. J. *Adv. Drug Delivery Rev.* **2005**, *57*, 1875–1889. (c) Haupt, K. *Chem. Commun.* **2003**, 171–178.
- (13) Some selected examples: (a) Turkewitsch, P.; Wandelt, B.; Darling, G. D.; Powell, W. S. *Anal. Chem.* **1998**, *70*, 2025–2030. (b) Manesiotis, P.; Hall, A. J.; Emgenbroich, M.; Quaglia, M.; De Lorenzi, E.; Sellergren, B. *Chem. Commun.* **2004**, 2278–2279. (c) Takeuchi, T.; Mukawa, T.; Matsui, J.; Higashi, M.; Shimizu, K. D. *Anal. Chem.* **2001**, *73*, 3869–3874. (d) Rathbone, D. L.; Bains, A. *Biosens. Bioelectron.* **2005**, *20*, 1438–1442. (e) Henry, O. Y. F.; Cullen, D. C.; Piletsky, S. A. *Anal. Bioanal. Chem.* **2005**, *382*, 947–956. (f) Matsui, J.; Higashi, M.; Takeuchi, T. *J. Am. Chem. Soc.* **2000**, *122*, 5218–5219.
- (14) Bidan, G.; Divisia-Blohorn, B.; Lapkowski, M.; Kern, J.-M.; Sauvage, J.-P. *J. Am. Chem. Soc.* **1992**, *114*, 5986–5994.

- (15) Some recent references: (a) Namvar, A.; Warriner, K. *Biosens. Bioelectron.* **2007**, *22*, 2018–2024. (b) Ramanavičius, A.; Ramanavičiene, A.; Malinauskas, A. *Electrochim. Acta* **2006**, *51*, 6025–6037. (c) Shiigi, H.; Kijima, D.; Ikenaga, Y.; Hori, K.; Fukazawa, S.; Nagaoka, T. *Electrochem. Soc.* **2005**, *152*, H129–H134. (d) Ho, K.-C.; Yeh, W.-M.; Tung, T.-S.; Liao, J.-Y. *Anal. Chim. Acta* **2005**, *542*, 90–96. (e) Panasyuk, T. L.; Mirsky, V. M.; Piletsky, S. A.; Wolfbeis, O. S. *Anal. Chem.* **1999**, *71*, 4609–4613.
- (16) Other approaches to TNT detection using molecularly imprinted materials: (a) Gao, D.; Zhang, Z.; Wu, M.; Xie, C.; Guan, G.; Wang, D. *J. Am. Chem. Soc.* **2007**, *129*, 7859–7866. (b) Bunte, G.; Hürtten, J.; Pontius, H.; Hartlieb, K.; Krause, H. *Anal. Chim. Acta* **2007**, *591*, 49–56. (c) Walker, N. R.; Linman, M. J.; Timmers, M. M.; Dean, S. L.; Burkett, C. M.; Lloyd, J. A.; Keelor, J. D.; Baughman, B. M.; Edmiston, P. L. *Anal. Chim. Acta* **2007**, *593*, 82–91.
- (17) Moratti, S. C. In *Handbook of Conducting Polymers*, 2nd ed.; Skotheim, T. A., Elsenbaumer, R. L., Reynolds, J. R., Eds.; Marcel Dekker: New York, 1998; pp 343–361.
- (18) (a) Rose, A.; Zhu, Z.; Madigan, C. F.; Swager, T. M.; Bulović, V. *Nature* **2005**, *434*, 876–879. (b) Kim, Y.; Zhu, Z.; Swager, T. M. *J. Am. Chem. Soc.* **2004**, *126*, 452–453. (c) Chang, C.-P.; Chao, C.-Y.; Huang, J. H.; Li, A.-K.; Hsu, C.-S.; Lin, M.-S.; Hsieh, B. R.; Su, A.-C. *Synth. Met.* **2004**, *144*, 297–301.
- (19) (a) Hittinger, E.; Kokil, A.; Weder, C. *Angew. Chem., Int. Ed.* **2004**, *43*, 1808–1811. (b) Weder, C. *Chem. Commun.* **2005**, 5378–5389.
- (20) Terao, J.; Tang, A.; Michels, J. J.; Krivokapic, A.; Anderson, H. L. *Chem. Commun.* **2004**, 56–57.

Scheme 1. Synthesis of Monomers for Polymerization

^a Reagents and conditions: (a) I_2 , HIO_3 , aq. H_2SO_4 , reflux, 12 h; (b) BBR_3 , CH_2Cl_2 , 25 °C, 48 h, 42% over two steps; (c) R-OTs, KI (cat.), K_2CO_3 , 2-propanone, 100 °C, 48 h, 81%; (d) $\text{Me}_3\text{SiC}\equiv\text{CH}$, $\text{Pd}(\text{PPh}_3)_4$ (cat.), CuI (cat.), $i\text{-Pr}_2\text{NH}$ –toluene, 70 °C, 48 h; (e) KOH , MeOH , 25 °C, 40 min, 41% over two steps; (f) pinacolborane, ZrCp_2HCl (cat.), $\text{ClCH}_2\text{CH}_2\text{Cl}$, 65 °C, 72 h, 54%; (g) $t\text{-BuLi}$, THF, –75 °C, 1 h; (h) $(\text{CH}_2\text{O})_n$, –75 °C → 25 °C, 12 h, 72%; (i) DMAP, CH_2Cl_2 , 25 °C, 24 h, **11a** (80%), **11b** (70%).

but becomes highly efficient in the presence of a catalytic amount of ZrCp_2HCl ²¹ and can serve as a convenient and general method to access highly valuable *trans* bis-vinylboronates.

In designing an imprinted system, the judicious selection of the side groups on a conjugated backbone is highly important. In our case, an imprinted cavity is likely to be formed between separate PPV strands that are rigidly held together by cross-linking units rather than a single chain “wrapping” around the template (Figure 1A). Therefore, the flexible long-chain substituents could improve the fitting of the imprinted cavity to a template by getting entangled in the three-dimensional (3D) network during the polymerization. These “trapped” chains can possibly fill the small voids between the template and the cavity which cannot be filled by the growing rigid 3D conjugated framework, and they shall stay in place after template removal. Based on this consideration, we chose the diethylene glycol side groups for the present study. One extra advantage these side groups can offer is the possibility of stabilizing interactions between their ether oxygen atoms and electron-deficient core of the nitroaromatic analytes that could result in stronger binding between the analyte and the imprinted cavity.

(21) Pereira, S.; Srebnik, M. *Organometallics* **1995**, *14*, 3127–3128.

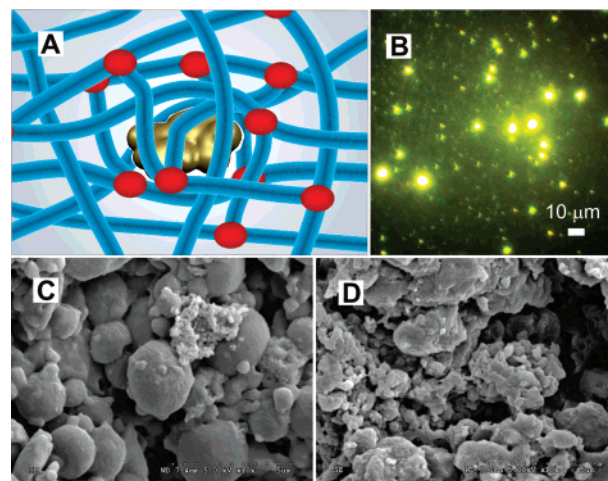


Figure 1. (A) Schematic representation of a template imprinted into a CP network. Red dots correspond to cross-linking units. (B) Fluorescent optical micrograph of polymer **P2** (suspension in dioxane, illuminated through a blue filter in the excitation channel). (C) Scanning Electron Microscopy (SEM) image of polymer **P1**. (D) SEM image of polymer **P2**. Note the highly porous, spongy morphology of **P2**.

One of the most challenging problems in the conventional procedures for molecularly imprinted materials preparation is postpolymerization removal of a template.²² This commonly demands harsh conditions and cannot be accomplished completely. Consequently, if an actual analyte capable of fluorescence quenching was used as a template, even a small residual amount would result in strong “self-quenching” thus significantly diminishing or even eliminating the analytical response of the system. A strategy to overcome this difficulty is to choose a nonquenching surrogate template which possesses a shape similar to that of the actual analyte. We chose 2,4,6-triisopropyltoluene **2a** as a nonquenching template for preparing a “TNT-imprinted” polymer due to the similarity between **2a**’s and TNT’s molecular shapes.²³ The template-bearing monomer **11a** was prepared following the route in Scheme 1.

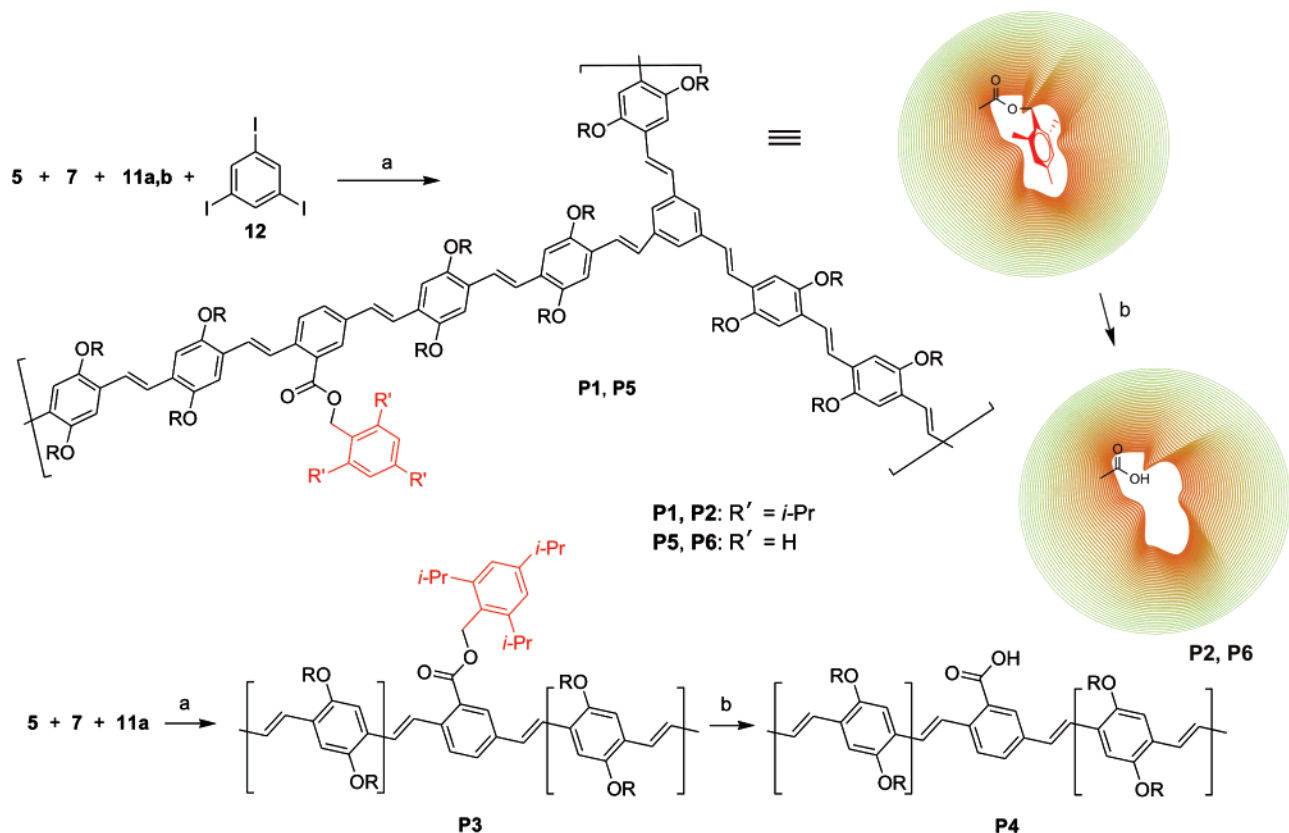
The polymerization of a mixture of comonomers **5** and **7**, the template-bearing monomer **11a** (10 mol %), and the cross-linker 1,3,5-triiodobenzene **12** (30 mol %) was carried out in a water–ethanol–toluene medium at high-speed stirring (~1000 rpm) in the presence of sodium dodecyl sulfate as a surfactant (Scheme 2).²⁴ This resulted in the cross-linked material **P1** as nonsoluble fluorescent spherically shaped micrometer-size particles. For comparison, we also carried out the polymerization under the same conditions but in the absence of the cross-linker **12** to yield the linear polymer **P3** that was soluble in common organic solvents. We then proceeded to find a suitable method to cleave the ester bond between the template and the polymer, in order to remove the template. After trying different approaches, we determined that lithium *n*-propyl mercaptide in HMPA worked the most efficiently.²⁵ Thus, the treatment of **P1** microparticles with an excess of this reagent at room

(22) (a) Ki, C. D.; Oh, C.; Oh, S.-G.; Chang, J. Y. *J. Am. Chem. Soc.* **2002**, *124*, 14838–14839. (b) Dirion, B.; Lanza, F.; Sellergren, B.; Chassaing, C.; Venn, R.; Berggren, C. *Chromatographia* **2002**, *56*, 237–241.

(23) Molecules **1** and **2a** show the opposite electrostatic potential distribution. Although this may result in differences in the template/analyte electrostatic interactions with the imprinted cavity, our experimental results demonstrated that the matching shape/size is a dominant factor.

(24) See Supporting Information for experimental details, procedures, and characterizations.

(25) Bartlett, P. A.; Johnson, W. S. *Tetrahedron Lett.* **1970**, 4459–4462.

Scheme 2. Synthesis and Structures of Polymers **P1–P6**

^a Reagents and conditions: (a) Pd(PPh₃)₄ (cat.), K₂CO₃, sodium dodecyl sulfate, H₂O–EtOH–toluene, 75 °C, 72 h; (b) *n*-PrSLi, HMPA, 25 °C, ultrasonication, 1.5 h, then HCl, MeOH.

temperature upon ultrasonication followed by extended washing with various solvents in a Soxhlet extractor yielded the highly fluorescent material **P2** (Figure 1B). Examination of **P2** with Scanning Electron Microscopy (SEM) revealed a highly porous, spongy morphology which greatly contrasts the smooth surface morphology of the precursor **P1** (Figure 1C and 1D). It is likely that the porous morphology of the material **P2** resulted from washing out the less cross-linked fraction of the polymer by HMPA, therefore effectively increasing the surface area and providing access to a larger number of imprinted cavities (*vide infra*). The extent of the template removal was determined by comparing the FT-IR spectra of polymers **P1** and **P2** (Figure 2). The spectra are identical, except for the band corresponding to the stretching carbonyl frequency. In **P1** this band appears at 1710 cm^{−1}, while in **P2** the presence of an additional band at 1722 cm^{−1} can be attributed to the conversion from ester to free carboxylic acid upon the cleavage of the template–polymer linkage. Based on the relative intensities of the two bands in **P2**, we could estimate that approximately 50% of the template was removed in this polymer. Similar postpolymerization treatment of the linear polymer **P3** with *n*-PrSLi in HMPA resulted in polymer **P4** showing virtually no residual template by ¹H NMR analysis.

For comparison purposes, and to further investigate the validity of our imprinting hypothesis, we also prepared a cross-linked polymer **P5**. This polymer was prepared based on the same monomers and reaction conditions as **P1** with the exception of using, instead of **11a**, the template-bearing monomer **11b** (Scheme 2). This allowed incorporating toluene **2b** as a “wrong”, smaller size template structurally similar to

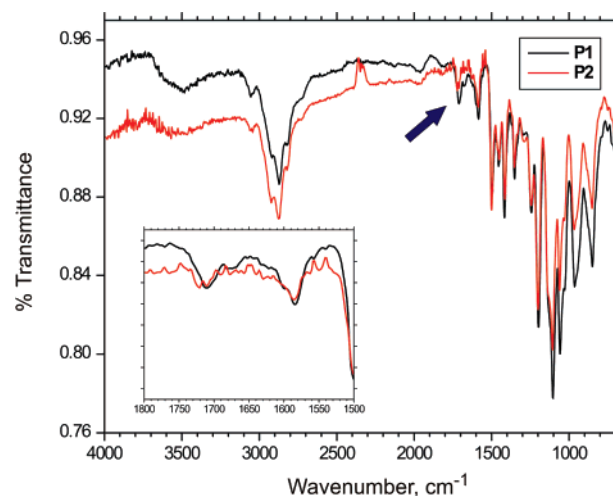


Figure 2. FT-IR spectra of polymers **P1** and **P2**. The carbonyl stretching frequency bands used to determine the extent of template removal are marked with a blue arrow, and the area around these bands is expanded in the inset. The frequency shift of the C=O band is ~12 cm^{−1}.

the “TNT-like” template **2a**. The corresponding MICP **P6** was obtained after removal of the template from **P5** using *n*-PrSLi in HMPA (Scheme 2). The FT-IR analysis similar to that described above revealed practically quantitative removal of the template in **P6** (Figure S1 in Supporting Information).

Photophysical Properties of the Polymers. Analysis of spectral properties of the obtained materials revealed a noticeable difference between the cross-linked (**P1**, **P2**, **P5**, and **P6**) and linear (**P3** and **P4**) polymers. The cross-linked materials display small hypsochromic shifts in both absorption and fluorescence

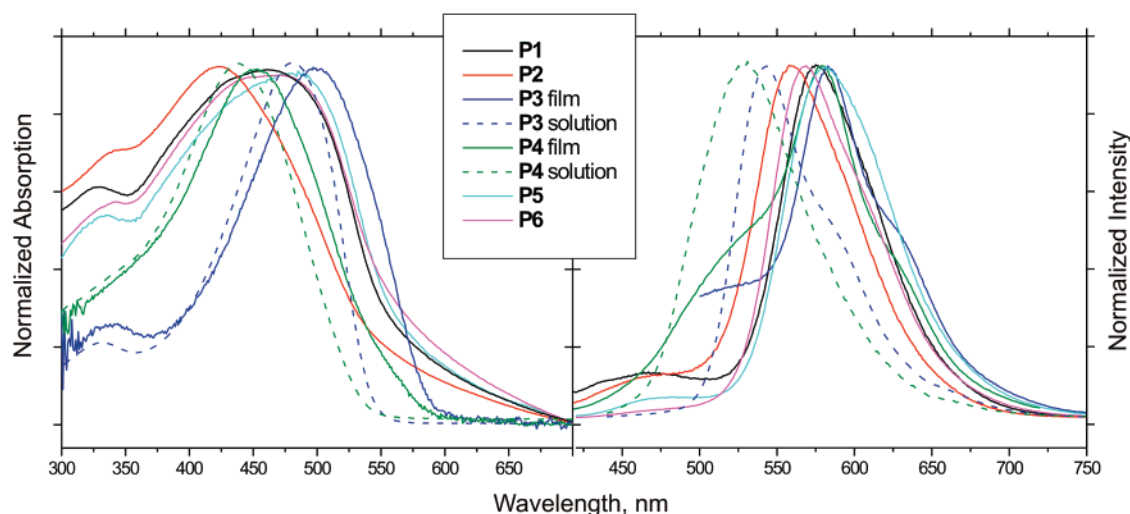


Figure 3. Absorption (left) and fluorescence (right) spectra of **P1–P6**. Dashed lines correspond to spectra in CH_2Cl_2 solution (for **P3**, **P4**); solid lines correspond to spectra acquired in spin-cast films. The absorption spectra for **P1**, **P2**, **P5**, and **P6** were acquired from suspensions in CHCl_3 . Extinction coefficients in solution (per repeating unit): **P3** $\epsilon(481 \text{ nm})$ 21 000, **P4** $\epsilon(439 \text{ nm})$ 13 000. Fluorescence quantum yields: **P1** ~ 0.03 , **P2** ~ 1.00 , **P3** 0.23 (solution), <0.001 (solid), **P4** 0.33 (solution), 0.007 (solid).

spectra relative to the linear analogues (Figure 3). This can be attributed to shorter π -electron conjugation in the former as the conjugation is diminished due to bending of the CP backbones to accommodate the template.²⁶

There is a noticeable spectral difference between the template-containing precursor (e.g., **P1**) and the MICP material (**P2**). Removal of the template resulted in substantial hypsochromic shifts both for the absorption ($\sim 40 \text{ nm}$ for **P1–P2** pair) and for the fluorescence bands ($\sim 20 \text{ nm}$ for **P1–P2** pair). This trend is quite consistent, does not seem to depend on the template (it also clearly showed up for the **P5–P6** pair), and therefore can be considered as a characteristic spectral signature of successful template removal. It is likely that this behavior reflects some reorganization of the polymer fragments adjacent to the imprinted cavity after the template is removed (possibly, even some collapsing of the cavity-forming CP inside the emptied imprinted cavity), resulting in decreasing conjugation length and attenuation of the exciton migration efficiency. With this assumption, one would expect seeing more drastic changes in the case of formation of a larger imprinted cavity as compared with formation of a smaller cavity. Indeed, this is the case for the related polymer pairs **P1–P2** and **P5–P6**. Removal of the substantially less bulky template **2b** in the latter case resulted in smaller spectral changes. While this interesting behavior definitely requires further investigation, it does serve as additional evidence in favor of the molecularly imprinted nature of polymers **P2** and **P6**.

Interestingly, molecularly imprinted polymer **P2** is highly emissive, with the fluorescence quantum yield approaching 100%. This remarkably increased emission efficiency can be attributed to a more rigid 3D conjugated framework which diminishes vibrationally/rotationally coupled electronic deactivation processes therefore reducing the rate of nonradiative decay.

Vapor-Phase Fluorescence Quenching. Exposure of **P1–P6** to saturated TNT vapors at room temperature resulted in

noticeable fluorescence quenching for all six polymers. In order to obtain quantitative characteristics of the quenching process to allow comparison of detection efficiency for the different polymers, vapor-phase Stern–Volmer experiments were carried out. In a typical Stern–Volmer experiment, a substrate is exposed to various concentrations of a quencher, and the drop in fluorescence intensity is described by eq 1:

$$\frac{I_0}{I} = 1 + K_{\text{SV}}[Q] \approx 1 + K'_{\text{SV}}t \quad (1)$$

In eq 1, I_0 is the initial fluorescence intensity without analyte, I is the fluorescence intensity with added analyte of concentration $[Q]$, and K_{SV} is the Stern–Volmer constant.²⁷ For gas-phase measurements, when a sample is exposed to an extremely low and steady concentration of an analyte vapor, and assuming that the quenching process is diffusion-controlled, the concentration of the analyte permeating into the sample and causing fluorescence quenching (equilibrium solubility) will be approximately proportional to the analyte's partial pressure (Henry's law).²⁸ With the steady pressure, the total amount of analyte absorbed by the sample should be proportional to the exposure time t , and therefore the time t can be used in quantitative experiments as a variable instead of the concentration $[Q]$ in the eq 1.²⁹ Although this assumption is only approximately valid, it allows running Stern–Volmer experiments for extra-low concentrations of gas-phase analytes using a relatively simple experimental setup. For our experiments, we used borosilicate glass slides with a layer of attached polymer microparticles prepared by spin-casting from their dilute suspensions in chloroform. The glass slides were placed inside a sealed quartz cuvette containing small amounts of various solid analytes deposited onto cotton gauze to ensure constant vapor pressure, and the cuvette was immediately placed into a fluorimeter to record the sample's fluorescence spectra at particular time intervals. A representative

(26) Alternatively, the decrease in conjugation length may be due to cross-conjugation in *meta*-substituted cross-linker units, which disrupts the π -electron conjugation in the ground state (but enhances the conjugation in the excited state; see: Thomson, A. L.; Gaab, K. M.; Xu, J.; Bardeen, C. J.; Martinez, T. J. *J. Phys. Chem. A* **2004**, *108*, 671–682). This effect requires further studies which will be reported elsewhere.

(27) Turro, N. J. *Modern Molecular Photochemistry*; University Science Books: Mill Valley, CA, 1991.

(28) Masoumi, Z.; Stoeva, V.; Yekta, A.; Pang, Z.; Manners, I.; Winnik, M. A. *Chem. Phys. Lett.* **1996**, *261*, 551–557.

(29) Note that the Stern–Volmer constants K_{SV} and K'_{SV} in eq 1 are different and are expressed in different units.

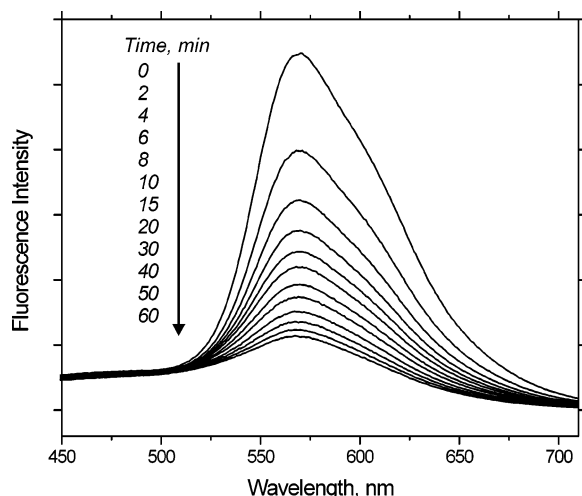


Figure 4. Quenching of fluorescence emission of polymer **P2** upon exposure to TNT vapors at room temperature at various time intervals.

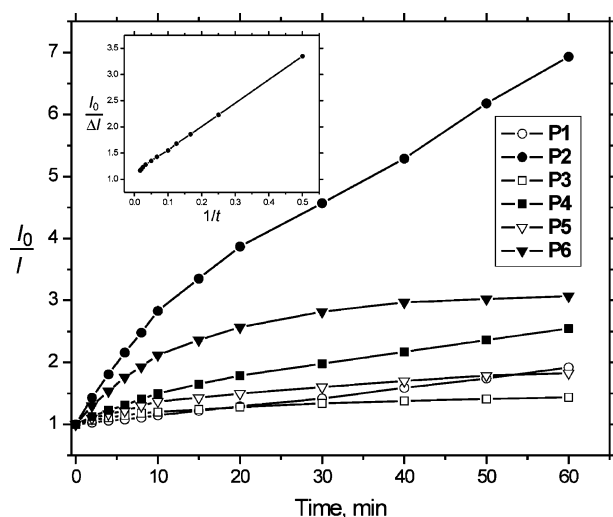


Figure 5. Stern–Volmer plots for polymers **P1–P6** fluorescence quenching with saturated vapors of TNT at room temperature. Inset: modified Stern–Volmer plot for polymer **P2**.

set of fluorescence spectra obtained in this way for the exposure of polymer **P2** to TNT vapors is shown in Figure 4.

The vapor-phase Stern–Volmer plots obtained for polymers **P1–P6** are shown in Figure 5. As expected, the “TNT-imprinted” polymer **P2** showed better sensitivity to TNT than its non-imprinted linear analogue **P4** or template-containing non-imprinted precursors **P1**, **P3**, and **P5**. An extremely important finding was that polymer **P6** imprinted with the “wrong” template also showed lower sensitivity to TNT. From these observations, we could conclude that the enhanced sensitivity of **P2** is consistent with its “TNT-imprinted” nature, where the complementary imprinted cavities provide better recognition for TNT as compared to the other polymers with no imprinted cavities (**P1**, **P3–P5**) or with substantially smaller size, “wrong” imprinted cavities (**P6**). The Stern–Volmer plot for polymer **P2** initially shows a linear behavior consistent with the eq 1; however, upon longer exposure it displays downward curvature (Figure 5). The downward curvature is likely to reflect a saturation phenomenon, when the analyte first permeates into easily accessible imprinted cavities (linear part of the plot), which is followed by much slower absorption into less accessible cavities. With a very approximate assumption that only two

types of cavities are present, such a behavior can be analyzed using the modified Stern–Volmer equation:³⁰

$$\frac{I_0}{\Delta I} = \frac{1}{f_a} + \frac{1}{f_a K_{SV}^a [Q]} \quad (2)$$

In eq 2, I_0 is the initial fluorescence intensity without analyte, $\Delta I = I_0 - I$ is the fluorescence intensity drop with added analyte of concentration $[Q]$, f_a is the fraction of easily accessible cavities, and K_{SV}^a is the Stern–Volmer constant for quenching inside these cavities. A plot in the coordinates from eq 2 is shown as an inset to Figure 5. Its linearity does agree with the proposed model of having two types of imprinted cavities. From this plot, the fraction of easily accessible cavities f_a was estimated to be 0.9. Although this value is very approximate and should be considered cautiously, it is in good agreement with the highly porous nature of polymer **P2**, when not only cavities close to the surface but also cavities well inside the polymer microparticles are accessible through the network of interconnecting channels. From a practical standpoint, this property is of ultimate significance for chemical sensing materials.

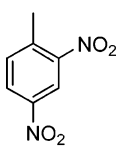
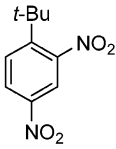
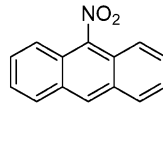
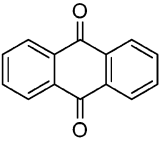

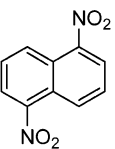
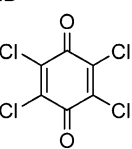
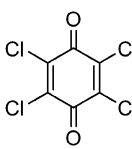
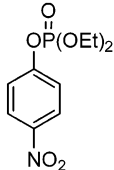
Analysis of TNT quenching data for polymers **P1–P6** (Figure 5) allows us to differentiate between fluorescence quenching due to selective recognition of the analyte by molecularly imprinted cavities and quenching by the analyte molecules nonselectively bound at the surface of the sensor material. In principle, the effect of such nonspecific surface associations with electron-deficient TNT can be significantly amplified by the efficient 3D exciton migration resulting in a noticeable nonselective fluorescence quenching. Indeed, it is this quenching mode which produces highly sensitive but not selective detection of electron-deficient analytes by the traditional non-imprinted CPs.⁶ In the case of template-containing precursor polymers **P1**, **P3**, and **P5**, as well as the spin-cast film of linear polymer **P4**, such nonspecific fluorescence quenching by surface-bound TNT is the primary quenching pathway; since the surface area is relatively small, the magnitude of the analytical response is noticeable but not significant.³¹ The template removal procedure produces a material with a highly porous morphology (Figures 1C and 1D). Due to the greater surface area, the increased probability of the analyte nonspecific binding is a possible reason for the overall enhanced quenching response of polymer **P6**, since selective recognition of TNT by **P6**’s much smaller imprinted cavity seems unlikely. It is natural to assume that the “TNT-imprinted” polymer **P2** which was prepared under conditions similar to those for **P6** would have exhibited a somewhat similar quenching efficiency had there been no specific recognition by imprinted cavities involved. Therefore, **P2**’s almost 2-fold higher quenching response upon TNT exposure (Figure 5) stems from the selective recognition of TNT due to molecular imprinting.

In order to further understand the distinguished behavior of **P2** and eliminate the possibility that this special behavior is simply due to the highly porous morphology of this material,

(30) Lakowicz, J. R. *Principles of Fluorescence Spectroscopy*, 3rd ed.; Springer: New York, 2006.

(31) Diffusion-controlled analyte penetration from the surface into the bulk of the solid material will depend on the solubility of the analyte in the polymer and may also affect the quenching efficiency, especially at longer exposure times. Still, considering the relative similarity between the polymers under study, it is expected to provide only a minor contribution.

Table 1. Structures and Properties of the Analytes Used in the Quenching Selectivity Studies^a

									
TNT	DNT	BDNB	NA	AQ	DNN	CA	DDQ	PO	
VP ^b	1	18	2 ^c	0.07	0.02	0.05	950	8	0.03
E _{Red} , V ^d	−0.77	−1.01	−0.99	−1.21	−0.97	−0.90	−0.05	0.61	−1.16
ΔG ₀ , eV	−0.91	−0.67	−0.69	−0.47	−0.71	−0.78	−1.63	−2.29	−0.52
K _{SV} (P2) ^e	1.0	3.50	0.56	0.28	0.56	0.33	0.83	0.39	0.28
K _{SV} (P1) ^e	0.11	0.39	0.11	0.11	0.11	0.06	0.44	0.11	0.22

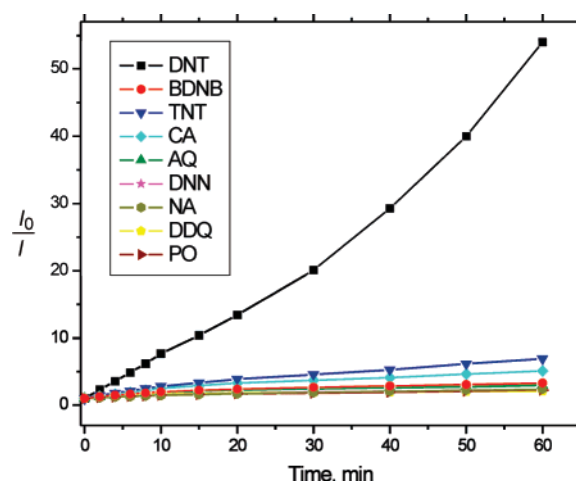
^a VP, equilibrium vapor pressure (relative to TNT); E_{Red}, electrochemical reduction potential (relative to SCE); ΔG^o, Gibbs free energy for the electron transfer from the polymer's excited state to a given quencher; K_{SV}(**P2**) and K_{SV}(**P1**), experimental Stern–Volmer constant for fluorescence quenching of polymers **P2** and **P1**, respectively (relative to TNT). ^bThe data from: *Handbook of Physical Properties of Organic Chemicals*; Howard, P. H., Meylan, W. M., Eds.; CRC Press: Boca Raton, FL, 1997. ^cEstimated by extrapolation. ^dExperimentally measured in CH₂Cl₂ solutions (0.1 M Bu₄NPF₆ as supporting electrolyte) with Pt working electrode. ^eDetermined from the slope of the initial straight sections of corresponding Stern–Volmer graphs.

we carried out a comparative study using a group of analytes with different molecular shapes and sizes which can interfere with TNT detection. These analytes are listed in Table 1 along with their corresponding equilibrium vapor pressure, reduction potential, and Gibbs free energy change (ΔG^o) for the electron transfer from the excited polymer to a particular quencher. Since fluorescence quenching involves an electron transfer from the excited polymer to the LUMO of a quencher, the magnitude of ΔG^o determines the thermodynamic “driving force” of the quenching process, and it was estimated using the Rehm–Weller equation:³²

$$\Delta G^{\circ} = E_{\text{Ox}}(\text{P/P}^{+\bullet}) - E_{\text{Red}}(\text{Q/Q}^{\bullet-}) - E_{00} \quad (3)$$

In this equation, E_{Ox}(P/P⁺), E_{Red}(Q/Q^{•−}), and E₀₀ are the oxidation potential of polymer **P2**, the reduction potential of a quencher, and the energy difference between ground and first excited singlet states of the polymer, respectively. As polymer **P2** was not soluble, we used the values determined for the related polymer **P4**. The value of E_{Ox}(P/P⁺) (0.82 V vs SCE) was determined electrochemically, and E₀₀ (2.5 eV) was obtained from the intersecting wavelength of the normalized absorption and fluorescence spectra. As can be seen from Table 1, the electron transfer is a highly exergonic process for each analyte, with the exergonicity being either comparable to that of TNT or significantly exceeding it. Therefore, if the quenching process was simply thermodynamically controlled (as in the case of nonspecific surface associations), each of these compounds would demonstrate similar or better quenching of **P2**'s fluorescence than TNT does.

The last two lines in Table 1 give the relative values of Stern–Volmer constant K_{SV} for the imprinted polymer **P2** and the non-imprinted precursor **P1** fluorescence quenching with different analytes. They correspond to the slopes of the initial straight sections of the gas-phase Stern–Volmer plots (shown in Figure

**Figure 6.** Stern–Volmer plots for polymer **P2** fluorescence quenching with saturated vapors of the analytes listed in Table 1 (at room temperature).

6) and can be used to quantify the selectivity of **P2**'s chemosensing response. The outcome of the quenching experiments was consistent with the preliminary expectations, with the majority of the analytes (including likely field-use interferents such as a common agricultural insecticide paraoxon (PO)) not interfering significantly with the polymer's fluorescence, and non-imprinted precursor polymer **P1** exhibiting much smaller quenching response (mostly due to the nonspecific analyte binding). It was not affected even by exposure to 2,3-dichloro-5,6-dicyano-1,4-benzoquinone (DDQ), despite the remarkably high exergonicity of the electron-transfer quenching for this analyte. This means that even when the electron transfer is favored from the thermodynamic standpoint (which is especially significant for DDQ), **P2**'s analytical response is strongly determined by the imprinting effect. The analytes with the size/shape not matching the imprinted template are not capable of entering the imprinted cavity and causing fluorescent quenching.³³

(32) Rehm, D.; Weller, A. *Isr. J. Chem.* **1970**, *8*, 259–271.

One remarkable and clearly unexpected observation was that exposure of **P2** to vapors of 2,4-dinitrotoluene (DNT) caused much stronger fluorescence quenching than even TNT (Figure 6). Moreover, a Stern–Volmer plot for the DNT quenching is practically linear over the entire time span of the experiment and does not show saturation behavior (downward curvature) typical for other analytes. Although DNT's vapor pressure at room temperature is higher than that of TNT, its ability to quench by an electron-transfer mechanism is substantially diminished as reflected in the corresponding ΔG° values. Furthermore, the non-imprinted precursor **P1** was only slightly affected by DNT exposure. Therefore, the magnitude of **P2**'s response to DNT clearly indicates that the imprinted cavity provides a better fit to this analyte. Two factors are probably responsible for this. First, the surrogate template **2a** used for “TNT imprinting” in **P2** does not perfectly match the TNT molecular shape. The second factor is likely to be related to partial collapsing of the imprinted cavity upon removing the template leading to decreasing the “free volume” of the cavity. The experimental reflection of such reorganization is also seen in the characteristic hypsochromic shifts of absorption and fluorescence maxima observed upon template removal (*vide supra*). As a result, DNT rather than target TNT seems to be the best match to the **P2**'s imprinted cavities. Contrarily, **P2**'s fluorescence was practically not affected by exposure to 1-*tert*-butyl-2,4-dinitrobenzene (BDNB) that was specially prepared to compare with DNT. Both DNT and BDNB possess similar ΔG° values for electron transfer (Table 1); therefore the influence of electronic factors on quenching selectivity is almost negligible. Thus, the dramatic difference in the magnitude of fluorescence quenching by these two analytes can only be understood in terms of the molecularly imprinted nature of polymer **P2**, when the bulkier *tert*-butyl group in BDNB makes entering the imprinted cavity practically impossible.

It is important to mention that the molecularly imprinted polymer **P2** is remarkably air-stable and photostable. The polymer microparticles covered glass slides prepared for the experiments described herein were stored in air for 3 months without significant diminishing of their fluorescence intensity. This high stability greatly contrasts with the low stability of the linear analogue **P4**; thin films of **P4** degrade and become completely nonemissive after only a few hours of exposure to air. Absorption of DNT and TNT by **P2** is also completely reversible (Figure 7). Exposure of this polymer to DNT or TNT vapors for 10 min causes a substantial decrease in fluorescence intensity (almost complete for DNT); however, the fluorescence of the samples markedly recovers after keeping them for 10 min in air; the fluorescence recovers completely in 1 h. Such exposure to the quenchers with subsequent recovery of fluorescence can be done repeatedly, without any noticeable irreversible quenching. In contrast, thin films of the linear polymer **P4** become irreversibly quenched upon exposure to

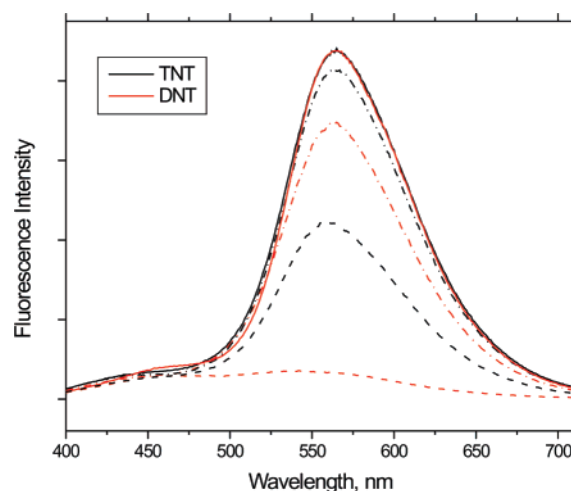


Figure 7. Quenching and recovery of fluorescence of **P2** with TNT and DNT. Solid line: initial fluorescence. Dash line: fluorescence immediately after 10 min of exposure to TNT (DNT) vapors. Dash-and-dot line: recovery of fluorescence after 10 min of exposure to air. Fluorescence of both samples was completely recovered after 1 h of exposure to air.

DNT or TNT (this irreversible quenching also coincides with irreversible oxidative degradation by air). This stability and analytical response reversibility increase the value of cross-linked molecularly imprinted conjugated polymers for potential chemosensing applications.

Conclusions

We demonstrated the principle possibility of molecular imprinting in three dimensionally cross-linked fluorescent conjugated polymers. The imprinting effect that is based on analyte shape/size recognition is substantial, although it is not capable of completely overriding the effect of nonspecific surface binding of electron-deficient analytes. Nevertheless, the new molecularly imprinted fluorescent conjugated polymer materials, as intrinsically amplifying signal transducers, are advantageous for sensing applications due to the ability to “program” the required detection selectivity through a choice of imprinted templates. While in the current study the “TNT-imprinted” material turned out to be a much better sensor for DNT, it may be possible to improve the fitness of the imprinted cavity to TNT by fine-tuning the surrogate imprinting template. Further experimental studies on various factors capable of influencing the imprinting effect, as well as gaining a deeper understanding of the nature and origin of this phenomenon, are required to optimize the performance of these materials and are currently underway.

Acknowledgment. This research was supported by the National Science Foundation (CAREER Award CHE-0547895), Louisiana Board of Regents (LEQSF Pfund-45), and LSU through start-up funding. Kind appreciation is due to Dr. W. Ong for helping with electrochemical measurements.

Supporting Information Available: Detailed synthetic and experimental procedures and additional data. This material is available free of charge via the Internet at <http://pubs.acs.org>.

JA0748027

(33) The anomalously high sensitivity of **P2** to chloranil (CA) can be explained by a combination of very high exergonicity for the electron transfer quenching and significantly (10^3 compared to TNT) higher vapor pressure. In addition, CA's shape and size are somewhat close to those of TNT which allows this compound to enter some of the more easily accessible imprinted cavities.